

RESEARCH ARTICLE

Synthesis of $M_{1-3x}Al_2O_4:Eu^{2+}_x/Dy^{3+}_{2x}$ ($M^{2+} = Sr^{2+}$, Ca^{2+} and Ba^{2+}) phosphors with long-lasting phosphorescence properties via co-precipitation method

Jinkai Li^{1†*} Bin Liu^{1†} Qi Chen¹ Yizhong Lu^{1*} Zongming Liu¹

Abstract: The long afterglow fluorescent material of $M_{1-3x}Al_2O_4:Eu^{2+}_x/Dy^{3+}_{2x}$ ($M^{2+} = Sr^{2+}$, Ca^{2+} and Ba^{2+}) phosphors are successfully synthesized by calcining precursor obtained via co-precipitation method at 1300°C for 4 h with reducing atmosphere (20% H_2 and 80% N_2). The phase evolution, morphology and afterglow fluorescent properties are systematically studied by the various instruments of XRD, FE-SEM, PLE/PL spectroscopy and fluorescence decay analysis. The PL spectra shows that the $Sr_{1-3x}Al_2O_4:Eu^{2+}_x/Dy^{3+}_{2x}$ phosphors display vivid green emission at ~519 nm ($4f^65d^1 \rightarrow 4f^7$ transition of Eu^{2+}) with monitoring of the maximum excitation wavelength at ~334 nm ($^8S_{7/2} \rightarrow ^6I_J$ transition of Eu^{2+}), among which the optimal concentration of Eu^{2+} and Dy^{3+} is 15 at.% and 30 at.%, respectively. The color coordinates and temperature of $Sr_{1-3x}Al_2O_4:Eu^{2+}_x/Dy^{3+}_{2x}$ phosphors are approximately at (~0.27, ~0.57) and ~6700 K, respectively. On the above basis, the $M_{0.55}Al_2O_4:Eu^{2+}_{0.15}/Dy^{3+}_{0.3}$ ($M^{2+} = Ca^{2+}$ and Ba^{2+}) phosphors is obtained by the same method. The PL spectra of these phosphors shows the strongest blue emission at ~440 nm and cyan emission at ~499 nm under ~334 nm wavelength excitation, respectively, which are blue shifted comparing to $Sr_{1-3x}Al_2O_4:Eu^{2+}_x/Dy^{3+}_{2x}$ phosphors. The color coordinates and temperatures of $M_{0.55}Al_2O_4:Eu^{2+}_{0.15}/Dy^{3+}_{0.3}$ ($M^{2+} = Ca^{2+}$ and Ba^{2+}) phosphors are approximately at (~0.18, ~0.09), ~2000 K and (~0.18, ~0.42), ~11600 K, respectively. In this work, long afterglow materials of green, blue and cyan aluminates phosphors with excellent properties have been prepared, in order to obtain wide application in the field of night automatic lighting and display.

Keywords: long afterglow material, co-precipitation method, $M_{1-3x}Al_2O_4:Eu^{2+}_x/Dy^{3+}_{2x}$ ($M^{2+} = Sr^{2+}$, Ca^{2+} and Ba^{2+}) phosphors, luminescent property

1 Introduction

Long afterglow phosphors, as a kind of special materials, can emit visible light after absorbing sunlight or artificial light sources and have been successfully applied in many fields^[1-3]. Previous studies demonstrate that aluminate (MA_2O_4) is a kind of satisfactory luminescent matrix due to its wide band gap. Compared with conventional sulphide phosphors (*e.g.*, ZnS), it shows better chemical stability^[4] and environmental friendliness^[5-8].

In addition, in MA_2O_4 matrix, the M^{2+} is located in the interior of $[AlO_4]^{5-}$ tetrahedral and occupies the position of two low symmetries and coordination^[9,10]. The defects based upon Eu^{2+} and Dy^{3+} ions doping are easily formed under such condition. In contrast to other matrices, such as MA_4O_7 , $MA_{12}O_{19}$, $M_4Al_{14}O_{25}$ and $M_2Al_6O_{11}$, the MA_2O_4 ($M^{2+} = Sr^{2+}$, Ca^{2+} and Ba^{2+}) phosphors have the highest luminescence intensity and longest afterglow time^[11-14]. Recently, MA_2O_4 doped with Eu^{2+} and Dy^{3+} ions as long afterglow phosphor, has been well accepted in biological sensing, plastic, coating, glass, textile, solar cell fields^[15-21].

In this paper, the $M_{1-3x}Al_2O_4:Eu^{2+}_x/Dy^{3+}_{2x}$ ($M^{2+} = Sr^{2+}$, Ca^{2+} and Ba^{2+}) phosphors have been successfully synthesized by co-precipitation method. Compared with the solid state reaction^[22], sol-gel^[23], auto-combustion^[24] and hydrothermal^[25] methods, the co-precipitation method has such advantages as precise control of raw materials and high purity of target sample^[26]. The phase evolution, morphologies and af-

Received: June 20, 2019 Accepted: July 6, 2019 Published: July 11, 2019

* Correspondence to: 1. Jinkai Li, School of Materials Science and Engineering, University of Jinan, Jinan, Shandong 250022, China; Email: mse.lijk@ujn.edu.cn; 2. Yizhong Lu, School of Materials Science and Engineering, University of Jinan, Jinan, Shandong 250022, China; Email: mse.luyz@ujn.edu.cn

† These authors contributed equally to this work.

Citation: Li J, Liu B, Chen Q, *et al.* Synthesis of $M_{1-3x}Al_2O_4:Eu^{2+}_x/Dy^{3+}_{2x}$ ($M^{2+} = Sr^{2+}$, Ca^{2+} and Ba^{2+}) phosphors with long-lasting phosphorescence properties via co-precipitation method. *Chem Rep*, 2019, 1(2): 112-117.

Copyright: © 2019 Jinkai Li, Yizhong Lu, *et al.* This is an open access article distributed under the terms of the [Creative Commons Attribution License](https://creativecommons.org/licenses/by/4.0/), which permits unrestricted use, distribution, and reproduction in any medium, provided the original author and source are credited.

terglow fluorescent properties of samples are investigated by XRD, FE-SEM, PLE/PL spectroscopy and fluorescence decay analysis. In the following, we systematically displayed the results of the discussion for the $M_{1-3x}Al_2O_4 \cdot Eu^{2+}_x/Dy^{3+}_{2x}$ ($M^{2+} = Sr^{2+}, Ca^{2+}$ and Ba^{2+}) phosphors about the phase evolution, morphologies, and fluorescent properties.

2 Experiment procedure

2.1 Materials

In a study, strontium nitrate ($Sr(NO_3)_2$, AR, Tianjin Guangcheng Chemical Reagent Co., Ltd. Tianjin, china), calcium nitrate ($Ca(NO_3)_2$, AR, Tianjin Damao Chemical Reagent Factory, Tianjin, china), barium nitrate ($Ba(NO_3)_2$, AR, Sinopharm Chemical Reagent Co. Ltd., Shanghai, China), aluminum nitrate ($Al(NO_3)_3 \cdot 9H_2O$, 99.0%, Sinopharm Chemical Reagent Co. Ltd., Shanghai, China), Dy_2O_3 (99.99%, Huizhou Ruier Rare Chemical Hi-Tech Co. Ltd., Huizhou, China urea), Eu_2O_3 (99.999%, Huizhou Ruier Rare Chemical Hi-Tech Co. Ltd., Huizhou, China urea), ammonium hydrogen carbonate (AHC, NH_4HCO_3 , AR, Sinopharm Chemical Reagent Co., Ltd., Shanghai, China) ethylene glycol (EG, $HOCH_2CH_2OH$, >99%, Tianjin City Fuyu Fine Chemical Co. Ltd., Tianjin, China), and nitric acid (AR, Sinopharm Chemical Reagent Co. Ltd., Shanghai, China), were used as the raw material in the synthesis process.

2.2 Preparation procedure

The Eu_2O_3 and Dy_2O_3 were respectively dissolved in hot nitric acid, and were disposed at a certain concentration of rare earth nitrates $RE(NO_3)_3$ ($RE = Eu^{3+}$ and Dy^{3+}). The $M(NO_3)_2$ ($M^{2+} = Sr^{2+}, Ca^{2+}$ or Ba^{2+}), $Al(NO_3)_3 \cdot 9H_2O$, $Dy(NO_3)_3$ and $Eu(NO_3)_3$ were mixed based upon the chemical formula of $M_{1-3x}Al_2O_4 \cdot Eu^{2+}_x/Dy^{3+}_{2x}$. In all the case, carbonate precursors were precipitated while the fully mixed mother salts were dropped in 1.5M ammonium hydrogen carbonate (NH_4HCO_3) at the speed of 5 mL/min. After aging reaction for 30 minutes, carbonate precursors were centrifuged and washed repeatedly with distilled water and alcohol to remove by-products. The wet precipitate was dried in air at $80^\circ C$ for 24 h. Finally, they were calcined at $1300^\circ C$ reducing atmosphere (20% H_2 and 80% N_2) to obtain the samples.

2.3 Characterization

The phase composition analysis was performed by XRD. And the patterns were recorded at room tempera-

ture using nickel-filtered $CuK\alpha$ radiation in the 2θ range $10-50^\circ$ at a scanning speed of $4.0^\circ 2\theta/min$ (Model D8 ADVANCE, BRUKER Co., Germany). The morphology of the precursor and resultant products were gathered via FE-SEM (QUANTA FEG 250, FEI Co., America) with an acceleration voltage of 10 kV. Characterization of groups in precursors and calcined products were performed by FT-IR spectroscopy via the standard KBr method (Spectrum RXI, Perkin-Elmer, Shelton, CT). The photoluminescence excitation (PLE) and photoluminescence (PL) spectra were obtained using a Fluorescence Spectrophotometer (FP-6500, JASCO Co., Japan) at room temperature equipped with a $\Phi 60$ -mm integrating sphere (ISF-513, JASCO, Tokyo, Japan) and a 150-W Xe-lamp was used as excitation source. The optical performances for all samples were conducted under identical conditions with the slit breadth of 5 nm. The phosphor powder was excited with a selected wavelength and the intensity of the intended emission was recorded as a function of elapsed time after the excitation light was automatically cut-off using a shutter.

3 Results and discussion

The FE-SEM morphologies of $Sr_{1-3x}Al_2O_4 \cdot Eu^{2+}_x/Dy^{3+}_{2x}$ precursors and its phosphor calcined at $1300^\circ C$ with reducing atmosphere are shown in Figure 1a,b. It can be seen that its morphology is well dispersed and irregular in particle size. However, the particles tend to be larger after being calcined at $1300^\circ C$ with reducing atmosphere. The specific surface area of the phosphor powder is correspondingly increased and the number of traps on the surface of the particles is increased. The curves (1) and (2) in Figure 1c show the XRD pattern of $SrAl_2O_4$ pure phase and $Sr_{1-3x}Al_2O_4 \cdot Eu^{2+}_x/Dy^{3+}_{2x}$ phosphor, respectively. The calcined phosphor shows good crystallinity and well matched to XRD characteristic peaks of $SrAl_2O_4$ (JCPDS NO. 74-0794). In addition, it illustrates that the co-doped of Eu^{2+} and Dy^{3+} does not significantly change in the bulk structure, and

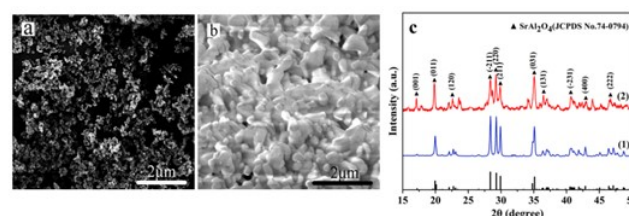


Figure 1. The FE-SEM morphologies of the $Sr_{1-3x}Al_2O_4 \cdot Eu^{2+}_x/Dy^{3+}_{2x}$ ($x=0.15$) precursor (a) and calcined phosphor (b), (c) is the XRD patterns of the $SrAl_2O_4$ matrix (1) and $Sr_{1-3x}Al_2O_4 \cdot Eu^{2+}_x/Dy^{3+}_{2x}$ ($x=0.15$) phosphor (2)

the SrAl_2O_4 matrix still retains a pure monoclinic crystal structure with space group $P2_1$.

Figure 2a,b show the photoluminescence excitation (PLE) and photoluminescence (PL) spectra of $\text{Sr}_{1-3x}\text{Al}_2\text{O}_4:\text{Eu}^{2+}_x/\text{Dy}^{3+}_{2x}$ phosphors with being doped with different concentrations of Eu^{2+} and Dy^{3+} ($x=0.05-0.3$), respectively. Monitoring the emission wavelength at 519 nm, the typical excitation bands of Eu^{2+} ions at 334 nm and 360 nm refer to $^8\text{S}_{7/2} \rightarrow ^6\text{I}_J$ and $^8\text{S}_{7/2} \rightarrow ^6\text{P}_7$ among the maximum excitation peak at 334 nm. Moreover, the other excitation band at 372 nm ($^6\text{P}_{7/2} \rightarrow ^8\text{S}_{7/2}$) belongs to a weak phonon companion [27–29]. Under the maximum excitation wavelength at 334 nm, it can be seen that the phosphors appear as a single green emission of Eu^{2+} ions at 519 nm ($4\text{f}^65\text{d}^1 \rightarrow 4\text{f}^7$) and without the emission peak of Dy^{3+} [27–29]. This is due to the fact that the doped of Dy^{3+} ions as auxiliary activators is mainly used to increase the number of defects and trap depth in the matrix, which can enhance the luminescence intensity and lifetime of Eu^{2+} ions. The emission intensity of Eu^{2+} increased with the Eu^{2+} doping up to $x=0.15$ ($x=15$ at.%), and then decreased owing to the concentration quenching (the inset of Figure 2b). The reason can be explained that the trap depth gradually increases leading to decrease the ability of photons to break free from traps, when the concentration of Eu^{2+} raised. Thus, the optimum doping amount of Eu^{2+} is 15 at%, which is similar to the tendency changed of the photoluminescence excitation spectra.

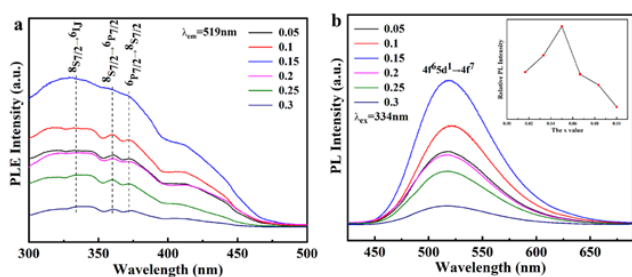


Figure 2. The PLE (a) and PL (b) spectrum of $\text{Sr}_{1-3x}\text{Al}_2\text{O}_4:\text{Eu}^{2+}_x/\text{Dy}^{3+}_{2x}$ precursors calcined at 1300°C with reducing atmosphere (20% H_2 and 80% N_2), the PLE spectra is obtained by monitoring the emission at 519 nm, while the PL spectra is depicted under the maximum excitation wavelength at 334 nm, the inset of Figure 2b shows the luminescence intensities changed with the concentration of Eu^{2+} gradually increased from 0.05 to 0.3

Figure 3 shows the Commission International de L'Eclairage (CIE) chromaticity coordinates for the emission of the all samples $\text{Sr}_{1-3x}\text{Al}_2\text{O}_4:\text{Eu}^{2+}_x/\text{Dy}^{3+}_{2x}$ under the excitation at 334 nm. From which it can be obtained that the color coordinate (x,y) and color temperature of all phosphors are ($\sim 0.27, \sim 0.56$), ~ 6749 K, ($\sim 0.28, \sim 0.57$), ~ 6508 K, ($\sim 0.27, \sim 0.57$), ~ 6714 K,

($\sim 0.28, \sim 0.57$), ~ 6508 K, ($\sim 0.27, \sim 0.55$), ~ 6786 K, ($\sim 0.27, \sim 0.55$), ~ 6786 K, respectively, with the Eu^{2+} fixed to $x=0.5, 1, 1.5, 2, 2.5, 3$, respectively, which the PL spectra of all samples analyzed and calculated, and thus emit a vivid green color.

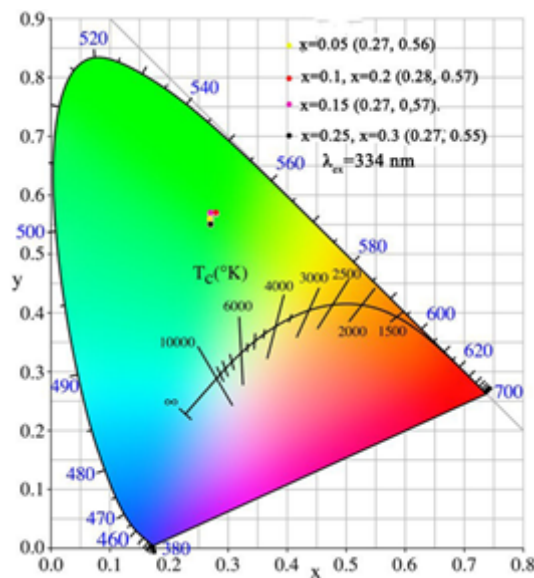


Figure 3. the Commission International de L'Eclairage (CIE) chromaticity coordinates for the emission of the all samples $\text{Sr}_{1-3x}\text{Al}_2\text{O}_4:\text{Eu}^{2+}_x/\text{Dy}^{3+}_{2x}$ ($x=0.05-0.3$) under the excitation at 334 nm

The afterglow decay is analyzed via double exponential fitting function characterization according to following the Equation (1) [30–32]:

$$I = A_1 \exp(-t/\tau_1) + A_2 \exp(-t/\tau_2) + B \quad (1)$$

where I is the luminescence intensity at a certain moment, t is the time, A_1, A_2 and B are constant, τ_1 and τ_2 show the time with the luminescence intensity rapidly and slowly weaken, respectively. Among them, the A_1, A_2, B, τ_1 and τ_2 are obtained from the double exponential fitting curve, and the effective decay time (τ) is calculated by the following Equation (2) [30–32]:

$$\tau = (A_1\tau_1^2 + A_2\tau_2^2)/(A_1\tau_1 + A_2\tau_2) \quad (2)$$

The decay curve for the 519 nm emission ($\lambda_{ex}=334$ nm) of the optimal sample of $\text{Sr}_{0.55}\text{Al}_2\text{O}_4:\text{Eu}^{2+}_{0.15}/\text{Dy}^{3+}_{0.3}$ is shown in Figure 4a. It can be obtained that the effective decay time (τ) is 25.333 ± 0.563 min, and A_1, A_2 and B are $2.784 \times 10^6 \pm 1.553 \times 10^5$ a.u., $1.987 \times 10^2 \pm 22.776$ a.u. and -0.144 ± 1.362 a.u., respectively. The result is similar to the digital photo under 365 nm UV excitation from a hand-held UV lamp for 10 min. (Figure 4b).

In order to further study the effect of matrix on

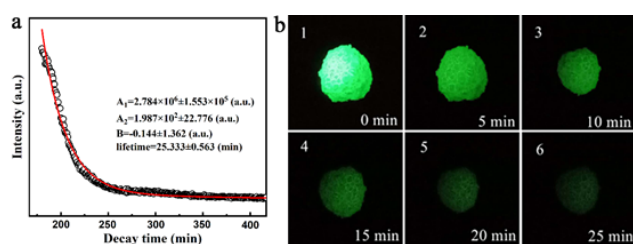


Figure 4. The decay curve of $Sr_{1-3x}Al_2O_4:Eu^{2+}_x/Dy^{3+}_{2x}$ ($x=0.15$) phosphor is shown in Figure 4a, Figure 4b depicts the digital picture of the luminescence intensities changed with the time increasing under 365 nm UV excitation from a hand-held UV lamp for 10 min

long-lasting fluorescence performance, Figure 5 shows the FE-SEM morphology particles of $M_{0.55}Al_2O_4:Eu^{2+}_{0.15}/Dy^{3+}_{0.3}$ precursor among which the M^{2+} refers to Ca^{2+} (Figure 5a), Sr^{2+} (Figure 5b) and Ba^{2+} (Figure 5c) respectively. It can be obtained that the modified matrix has no significant effect on the morphology of the particles with similar particle size and dispersibility.

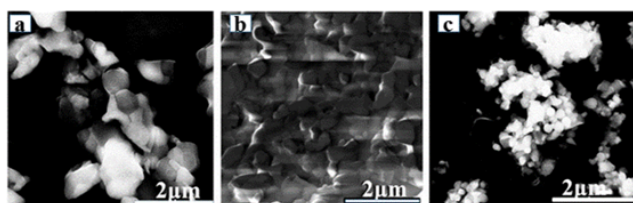


Figure 5. The FE-SEM morphology particle of $M_{0.55}Al_2O_4:Eu^{2+}_{0.15}/Dy^{3+}_{0.3}$ precursor among which the M^{2+} refers to Ca^{2+} (a), Sr^{2+} (b) and Ba^{2+} (c), respectively

The PLE and PL spectra of $M_{0.55}Al_2O_4:Eu^{2+}_{0.15}/Dy^{3+}_{0.3}$ ($M^{2+} = Ca^{2+}, Ba^{2+}$ and Sr^{2+}) are shown in Figure 6. In Figure 6a, the PLE spectra of $M_{0.55}Al_2O_4:Eu^{2+}_{0.15}/Dy^{3+}_{0.3}$ ($M^{2+} = Ca^{2+}, Ba^{2+}$ and Sr^{2+}) contains all Eu^{2+} ions excitation bands. Though the matrix changes, the maximum excitation peak position is still at 334 nm ($^8S_{7/2} \rightarrow ^6I_J$ transition of Eu^{2+}). Monitoring at 334 nm (Figure 6b), the PL spectra of $M_{0.55}Al_2O_4:Eu^{2+}_{0.15}/Dy^{3+}_{0.3}$ ($M^{2+} = Ca^{2+}, Ba^{2+}$ and Sr^{2+}) emit vivid blue (440 nm), cyan (499 nm) and green (519 nm) color, respectively. It is attributed to the fact that the radius of Ca^{2+} (1.000 Å), Ba^{2+} (1.350 Å) and Sr^{2+} (1.180 Å) are unlike to Eu^{2+} (1.170 Å) which results in lattice distortion with the Eu^{2+} doped, and thus, the color appears blue shift.

The Commission International de L'Eclairage (CIE) chromaticity coordinates for the emission of the $M_{0.55}Al_2O_4:Eu^{2+}_{0.15}/Dy^{3+}_{0.3}$ ($M^{2+} = Ca^{2+}$ and Ba^{2+}) under the excitation at 334 nm is shown in Figure 7. It can be seen that the color coordinate (x, y) and color temperature of $M_{0.55}Al_2O_4:Eu^{2+}_{0.15}/Dy^{3+}_{0.3}$ ($M^{2+} = Ca^{2+}$

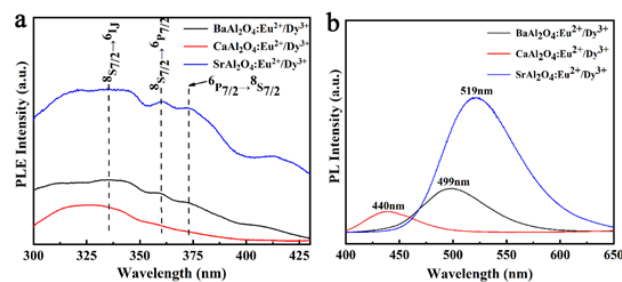


Figure 6. The PLE (a) and PL (b) spectrum of the $M_{0.55}Al_2O_4:Eu^{2+}_{0.15}/Dy^{3+}_{0.3}$ ($M^{2+} = Sr^{2+}, Ca^{2+}$ and Ba^{2+}) phosphors, among which the PL spectra is obtained by monitoring the 334 nm excitation

and Ba^{2+}) phosphors are ($\sim 0.18, \sim 0.09$), ~ 2000 K and ($\sim 0.18, \sim 0.42$), ~ 11600 K, respectively. And the blue and cyan colors of the $M_{0.55}Al_2O_4:Eu^{2+}_{0.15}/Dy^{3+}_{0.3}$ ($M^{2+} = Ca^{2+}$ and Ba^{2+}) phosphors, are seen from the digital pictures under 365 nm UV excitation from a hand-held UV lamp (the inset of Figure 7), which proves the results for the PL spectra shown in Figure 6b.

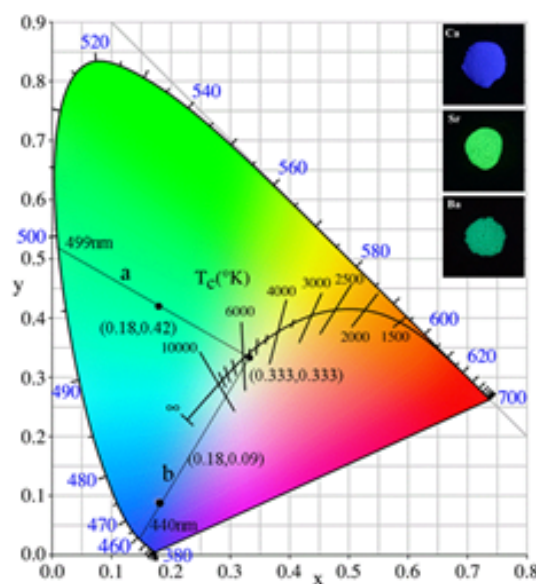


Figure 7. The Commission International de L'Eclairage (CIE) chromaticity coordinates for the emission of the $M_{0.55}Al_2O_4:Eu^{2+}_{0.15}/Dy^{3+}_{0.3}$ ($M^{2+} = Ca^{2+}$ and Ba^{2+}) phosphors under the excitation at 334 nm, the inset Figure 7 shows the digital picture of $M_{0.55}Al_2O_4:Eu^{2+}_{0.15}/Dy^{3+}_{0.3}$ ($M^{2+} = Ca^{2+}, Sr^{2+}$ and Ba^{2+}) phosphors under 365 nm UV excitation from a hand-held UV lamp

The investigation of phosphorescence lifetime decay behavior of long afterglow materials is an essential factor to study the changes of fluorescence properties. Figure 8 shows the decay curves of $M_{0.55}Al_2O_4:Eu^{2+}_{0.15}/Dy^{3+}_{0.3}$ ($M^{2+} = Ca^{2+}$ and Ba^{2+}) phosphors which are monitored at 440 nm and 499 nm, respectively. It can be seen that the effective decay time (τ) of

$M_{0.55}Al_2O_4:Eu^{2+}_{0.15}/Dy^{3+}_{0.3}$ ($M^{2+} = Ca^{2+}$ and Ba^{2+}) are 23.095 ± 0.174 min (Figure 8a) and 31.596 ± 0.839 min (Figure 8b), respectively. The reason for the decay time gradually increased with the radius increasing from Ca^{2+} to Ba^{2+} , is that the lattice shrinks more severe results in the defect depth increasing with the radius gradually increases, then the decay time gradually increased.

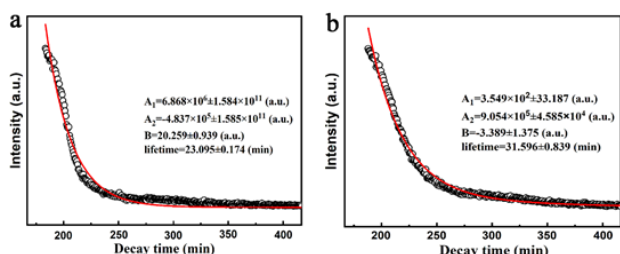


Figure 8. The decay curves of $M_{0.55}Al_2O_4:Eu^{2+}_{0.15}/Dy^{3+}_{0.3}$ ($M^{2+} = Ca^{2+}$ and Ba^{2+}) phosphors, respectively

4 Conclusions

A series of $M_{1-3x}Al_2O_4:Eu^{2+}_x/Dy^{3+}_{2x}$ ($M^{2+} = Ca^{2+}$, Ba^{2+} and Sr^{2+}) phosphors have been synthesized successfully via co-precipitation method, followed by calcination at $1300^\circ C$ with reducing atmosphere (20% H_2 and 80% N_2). Detailed characterizations analyzed by using the techniques of XRD, FE-SEM, PLE/PL, fluorescence decay and quantum efficiency have obtained the follow main conclusion:

(1) The $Sr_{1-3x}Al_2O_4:Eu^{2+}_x/Dy^{3+}_{2x}$ phosphors could be obtained at $1300^\circ C$ with reducing atmosphere (20% H_2 and 80% N_2), and the 15 at % Eu^{2+} and 30 at % Dy^{3+} doped do not change the crystal structure of $SrAl_2O_4$ matrix. All samples emit vivid green color at 519 nm ($4f^65d^1 \rightarrow 4f^7$ transition of Eu^{2+}) monitoring the excitation at 334 nm ($^8S_{7/2} \rightarrow ^6I_J$ transition of Eu^{2+}).

(2) On the above basis, the $M_{0.55}Al_2O_4:Eu^{2+}_{0.15}/Dy^{3+}_{0.3}$ ($M^{2+} = Ca^{2+}$ and Ba^{2+}) phosphors have been obtained by using the same method. Its phosphors display the blue (440 nm) and cyan (499 nm) color under the excitation wavelength at 334 nm. Along with the radius increasing, the color appears the blue shift.

(3) The luminescent properties (PLE/PL, lifetime, etc.) of resultant phosphors extremely rely on the concentration of defect and the defect depth, etc.

Acknowledgements

This research is supported by the National Natural Science Foundation of China (No. 51602126), the National Key Research and Development Plan of China (No. 2016YFB0303505), China and University of Jinan

Postdoctoral Science Foundation (No. 2017M622118 and XBH1716), the 111 Project of International Corporation on Advanced Cement-based Materials (D17001).

References

- [1] Palilla FC, Levine AK and Tomkus MR. Fluorescent properties of alkaline earth aluminates of type MA_2O_4 activated by divalent europium. *Journal of Electrochemical Society*, 1968, **115**(6): 642-644. <https://doi.org/10.1149/1.2411379>
- [2] Akiyama M, Xu CN, Nonaka K, *et al.* Intense visible light emission from $SrAl_2O_6:Eu,Dy$. *Applied Physics Letters*, 1998, **73**(21): 3046-3048. <https://doi.org/10.1063/1.122667>
- [3] Matsuzawa T, Aoki Y, Takeuchi N, *et al.* A new long phosphorescent phosphor with high brightness $SrAl_2O_4:Eu^{2+}, Dy^{3+}$. *Journal of Electrochemical Society*, 1996, **143**(8): 2670-2673. <https://doi.org/10.1149/1.1837067>
- [4] Peng M and Hong G. Reduction from Eu^{3+} to Eu^{2+} in $BaAl_2O_4:Eu$ phosphor prepared in an oxidizing atmosphere and luminescent properties of $BaAl_2O_4:Eu$. *Journal of Luminescence*, 2007, **127**(2): 735-740. <https://doi.org/10.1016/j.jlumin.2007.04.012>
- [5] Chang C, Li W, Huang X, *et al.* Photoluminescence and afterglow behavior of Eu^{2+} , Dy^{3+} and Eu^{3+} , Dy^{3+} in $Sr_3Al_2O_6$ matrix. *Journal of Luminescence*, 2010, **130**(3): 347-350. <https://doi.org/10.1016/j.jlumin.2009.09.016>
- [6] Gheorghe C, Gheorghe L, Achim A, *et al.* Optical properties of Sm^{3+} doped strontium hexa-aluminate single crystals. *Journal of Alloys and Compounds*, 2015, **622**: 296-302. <https://doi.org/10.1016/j.jallcom.2014.10.033>
- [7] Lupei V, Lupei A, Gheorghe C, *et al.* Composition dependence of Pr^{3+} spectral characteristics in strontium lanthanum aluminate crystals. *Optical Materials*, 2007, **30**(1): 164-167. <https://doi.org/10.1016/j.optmat.2006.11.018>
- [8] Gu X, Fu R, Yang F, *et al.* Tailoring the photoluminescence properties of lanthanum strontium aluminate phosphors by controlling crystal field environment with fluorine ions. *Journal of Rare Earths*, 2016, **34**(11): 1089-1094. [https://doi.org/10.1016/S1002-0721\(16\)60139-4](https://doi.org/10.1016/S1002-0721(16)60139-4)
- [9] Singh VP, Rai SB, Mishra H, *et al.* Stabilization of high temperature hexagonal phase of $SrAl_2O_4$ at room temperature: role of ZnO. *Dalton Transactions*, 2014, **43**(14): 5309-5316. <https://doi.org/10.1039/c3dt52869c>
- [10] Hwang KS, Kang BA, Kim SD, *et al.* Cost-effective electrostatic-sprayed $SrAl_2O_4:Eu^{2+}$ phosphor coatings by using salted sol-gel derived solution. *Bulletin of Materials Science*, 2011, **34**(5): 1059-1062. <https://doi.org/10.1007/s12034-011-0128-y>
- [11] Preethi KRS, Lu C, Thirumalai J, *et al.* $SrAl_4O_7:Eu^{2+}$ nanocrystals: synthesis and fluorescence properties. *Journal of Physics D (Applied Physics)*, 2004, **37**(19): 2664-2669. <https://doi.org/10.1088/0022-3727/37/19/009>

- [12] Huang SH, Wang XJ, Chen BJ, *et al.* Photon cascade emission and quantum efficiency of the 3P_0 level in Pr^{3+} -doped $SrAl_2O_4$ system. *Journal of Luminescence*, 2003, **S102-103**: 344-348.
[https://doi.org/10.1016/S0022-2313\(02\)00527-6](https://doi.org/10.1016/S0022-2313(02)00527-6)
- [13] Zhong RX, Zhang JH, Zhang X, *et al.* Red phosphorescence in $Sr_4Al_{14}O_{25} : Cr^{3+}, Eu^{2+}, Dy^{3+}$ through persistent energy transfer. *Applied Physics Letters*, 2006, **88**(20): 2670.
<https://doi.org/10.1063/1.2205167>
- [14] Sasaki T, Fukushima J, Hayashi Y, *et al.* Synthesis and photoluminescence properties of a novel $Sr_2Al_6O_{11}:Mn^{4+}$ red phosphor prepared with a B_2O_3 flux. *Journal of Luminescence*, 2018, **194**: 446-451.
<https://doi.org/10.1016/j.jlumin.2017.10.076>
- [15] Chen R, Hu Y, Chen L, *et al.* Luminescent properties of a novel afterglow phosphor $Sr_3Al_2O_5C_{12}:Eu^{2+}, Ce^{3+}$. *Ceramics International*, 2014, **40**(6): 8229-8236.
<https://doi.org/10.1016/j.ceramint.2014.01.020>
- [16] Ueda J, Aishima K, Nishiura S, *et al.* Afterglow Luminescence in Ce^{3+} -Doped $Y_3Sc_2Ga_3O_{12}$ Ceramics. *Applied Physics Express*, 2011, **4**(4): 257-261.
<https://doi.org/10.1143/APEX.4.042602>
- [17] Wang W, Li J, Duan G, *et al.* Morphology/Size Effect on the Luminescence Properties of the $[(Y_xGd_{1-x}Dy_{0.02})_2O_3]$ Phosphor with Enhanced Yellow Emission. *Journal of Luminescence*, 2017, **192**: 1056-1064.
<https://doi.org/10.1016/j.jlumin.2017.07.046>
- [18] Wang W, Yang P, Cheng Z, *et al.* Patterning of red, green, and blue luminescent films based on $CaWO_4:Eu^{3+}$, $CaWO_4:Tb^{3+}$, and $CaWO_4$ phosphors via microcontact printing route. *ACS Applied Materials & Interfaces*, 2011, **3**(10): 3921-3928.
<https://doi.org/10.1021/am2008008>
- [19] Tang Y, Song H, Su Y, *et al.* Turn-on Persistent Luminescence Probe Based on Graphitic Carbon Nitride for Imaging Detection of Biothiols in Biological Fluids. *Analytical Chemistry*, 2013, **85**(24): 11876-11884.
<https://doi.org/10.1021/ac403517u>
- [20] Hosseini Z, Huang WK, Tsai CM, *et al.* Enhanced light harvesting with a reflective luminescent down-shifting layer for dye-sensitized solar cells. *ACS Applied Materials & Interfaces*, 2013, **5**(12): 5397-5402.
<https://doi.org/10.1021/am401584y>
- [21] Li JK, Teng X, Wang WZ, *et al.* Investigation on the preparation and luminescence property of $(Gd_{1-x}Dy_x)_2O_3$ ($x=0.01-0.10$) spherical phosphors. *Ceramics International*, 2017, **43**: 10166-10173.
<https://doi.org/10.1016/j.ceramint.2017.05.041>
- [22] Chang YL, Hsiang HI and Liang MT. Characterizations of Eu, Dy co-doped $SrAl_2O_4$ phosphors prepared by the solid-state reaction with B_2O_3 addition. *Journal of Alloys and Compounds*, 2008, **461**(1-2): 589-603.
<https://doi.org/10.1016/j.jallcom.2007.07.078>
- [23] Tang Z, Zhang F, Zhang Z, *et al.* Luminescent properties of $SrAl_2O_4 : Eu, Dy$ material prepared by the gel method. *Journal of the European Ceramic Society*, 2000, **20**(12): 2129-2132.
[https://doi.org/10.1016/S0955-2219\(00\)00092-3](https://doi.org/10.1016/S0955-2219(00)00092-3)
- [24] Peng T, Yang H, Pu X, *et al.* Combustion synthesis and photoluminescence of $SrAl_2O_4:Eu,Dy$ phosphor nanoparticles. *Materials Letters*, 2004, **58**(3-4): 352-356.
[https://doi.org/10.1016/S0167-577X\(03\)00499-3](https://doi.org/10.1016/S0167-577X(03)00499-3)
- [25] Kutty TRN, Jagannathan R and Rao RP. Luminescence of Eu^{2+} in strontium aluminates prepared by the hydrothermal method. *Materials Research Bulletin*, 1990, **25**(11): 1355-1362.
[https://doi.org/10.1016/0025-5408\(90\)90217-P](https://doi.org/10.1016/0025-5408(90)90217-P)
- [26] Shan W, Wu L, Tao N, *et al.* Optimization method for green $SrAl_2O_4, Dy^{3+}$ phosphors synthesized via co-precipitation route assisted by microwave irradiation using orthogonal experimental design. *Ceramics International*, 2015, **41**(10): 15034-15040.
<https://doi.org/10.1016/j.ceramint.2015.08.050>
- [27] Kumar A, Kedawat G, Kumar P, *et al.* Sunlight-activated Eu^{2+}/Dy^{3+} doped $SrAl_2O_4$ water resistant phosphorescent layer for optical displays and defence applications. *New Journal of Chemistry*, 2015, **39**: 3380-3387.
<https://doi.org/10.1039/C4NJ02333A>
- [28] Park BG. Characteristics of Eu^{2+}, Dy^{3+} -doped $SrAl_2O_4$ synthesized by hydrothermal reaction and its photocatalytic properties. *Journal of Materials Science*, 2018, **6**(2): 12-21.
<https://doi.org/10.4236/msce.2018.62002>
- [29] Hua XW, Yang H, Guo TT, *et al.* Preparation and properties of Eu and Dy co-doped strontium aluminate long afterglow nanomaterials. *Ceramics International*, 2018, **44**: 7535-7544.
<https://doi.org/10.1016/j.ceramint.2018.01.157>
- [30] Rupérez A, Ayala L and Laserna JJ. Double exponential phase plane method for decay analysis in room temperature phosphorimetry. *Spectrochimica Acta, Part A (Molecular Spectroscopy)*, 1992, **48**(4): 569-575.
[https://doi.org/10.1016/0584-8539\(92\)80048-2](https://doi.org/10.1016/0584-8539(92)80048-2)
- [31] Huang CH and Chen TM. A Novel Single-Composition Trichromatic White-Light $Ca_3Y(GaO)_3(BO_3)_4:Ce^{3+}, Mn^{2+}, Tb^{3+}$ Phosphor for UV-Light Emitting Diodes. *The Journal of Physical Chemistry C*, 2011, **115**(5): 2349-2355.
<https://doi.org/10.1021/jp107856d>
- [32] Li J, Li JG, Li X, *et al.* Photoluminescence properties of phosphors based on Lu^{3+} -stabilized $Gd_3Al_5O_{12}: Tb^{3+}/Ce^{3+}$ garnet solid solutions. *Optical Materials*, 2016, **62**: 328-334.
<https://doi.org/10.1016/j.optmat.2016.09.076>